Treatment-Induced Damage to the Tumor Microenvironment Promotes Prostate Cancer Therapy Resistance Through WNT16B

Yu Sun, Judith Campisi, Celestia Higano, Tomasz M. Beer, Peggy Porter, Isa Coleman, Lawrence True, and Peter S. Nelson

Supplementary Figures and Experimental Procedures

Sun et al Supplementary Figure 1

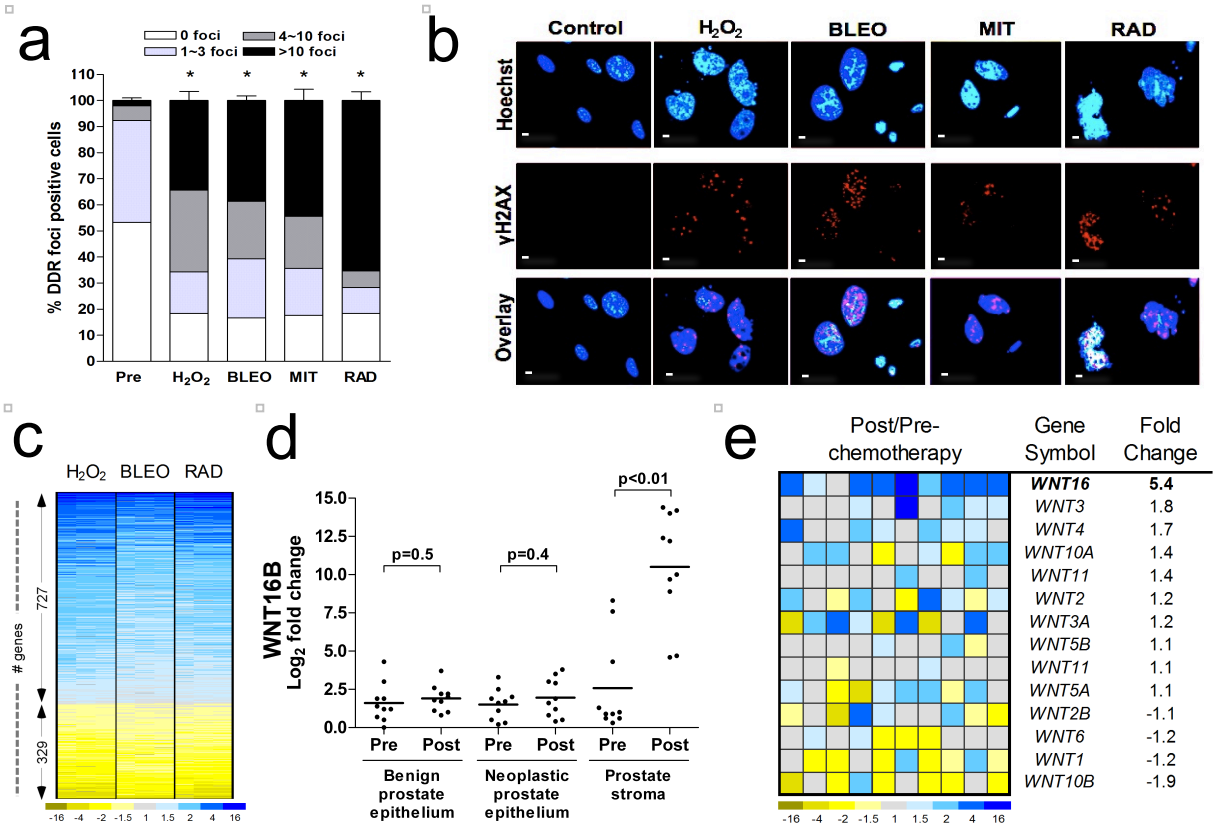

Supplementary Figure 1. Analysis of DNA damage responses (DDR) in prostate fibroblasts following DNA damaging cancer therapy. (**a)** Quantitation of DNA damage foci before (Pre) and after DNA damaging treatments. DDR foci identified by immunofluorescence staining for γ-H2AX (see Fig 1b) were recorded according to a 4-category scale. Data were averaged from readings of 3 independent fields, each with a total count of 100 nuclei. * represent significant differences $P < 0.01$ compared to untreated (Pre). **(b)** Analysis of DNA damage foci formation in prostate fibroblasts upon exposure to various DNA damaging agents. PSC27 prostate fibroblasts were treated with H_2O_2, bleomycin (BLEO) or gamma-irradiation (RAD). Immunofluorescence staining for γ-H2AX (red foci), with nuclei counterstained by Hoechst 33342 (Blue). Scale bar, 15 μm. **(c**) Analysis of gene expression changes in prostate fibroblasts by microarray hybridization. The heatmaps depict the relative mRNA levels after exposure to hydrogen peroxide (H_2O_2), Bleomycin (BLEO) or ionizing radiation (RAD) compared to vehicle treated cells. (red, increased; green, decreased following DNA damage). **(d)** WNT16B transcript levels in specific cell populations microdissected from prostate tissues before and after exposure to cytotoxic chemotherapy. Measurements are by qRT-PCR. Log_2 fold changes are shown relative to the lowest measurement of untreated benign prostate epithelium. Each data-point represents an individual patient sample.
(e) Transcript levels of WNT family members in microdissected human prostate stroma acquired before and after exposure to chemotherapy as quantitated by microarray hybridization. Columns represent individual patients. Values for each gene are mean-centered across all samples.

Sun et al
Supplementary Figure 2

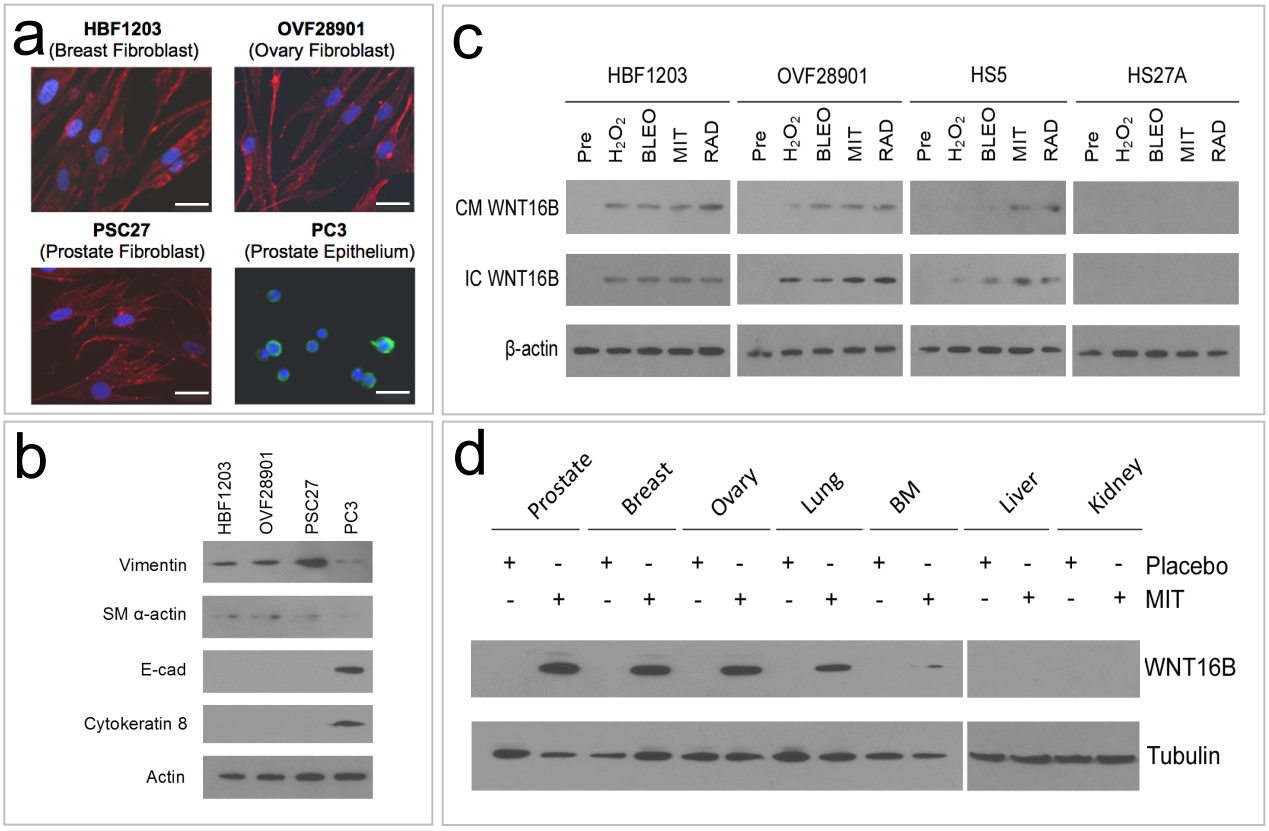

Supplementary Figure 2. DNA damage induces WNT16B expression in a spectrum of human fibroblasts and murine organs.
(a, b) Human prostate fibroblasts (HSP27), and newly derived breast (HBF1203) and ovarian (OVF28901) primary fibroblast lines express stromal but not epithelial markers. (a) Concurrent immunofluorescence staining using vimentin (red) and cytokeratin 8 (green) antibodies with PC3 cells serving as a positive control for epithelial cells. Scale bar, 15 μm. (b) Western immunoblot of stromal and epithelial cell lines confirming expression of mesenchymal and epithelial proteins, respectively.
(c) WNT16B expression is induced by DNA damage in most, but not all human fibroblast isolates: HBF1203 (breast), OVF28901 (ovary), HS5 (bone marrow) and HS27A (bone marrow). CM, conditioned media; IC, intracellular lysates.
(d) Systemic chemotherapy induces WNT16B expression in diverse murine organs. Each tissue type was collected after three mitoxantrone treatments administered over 8 weeks.

Sun et al Supplementary Figure 3

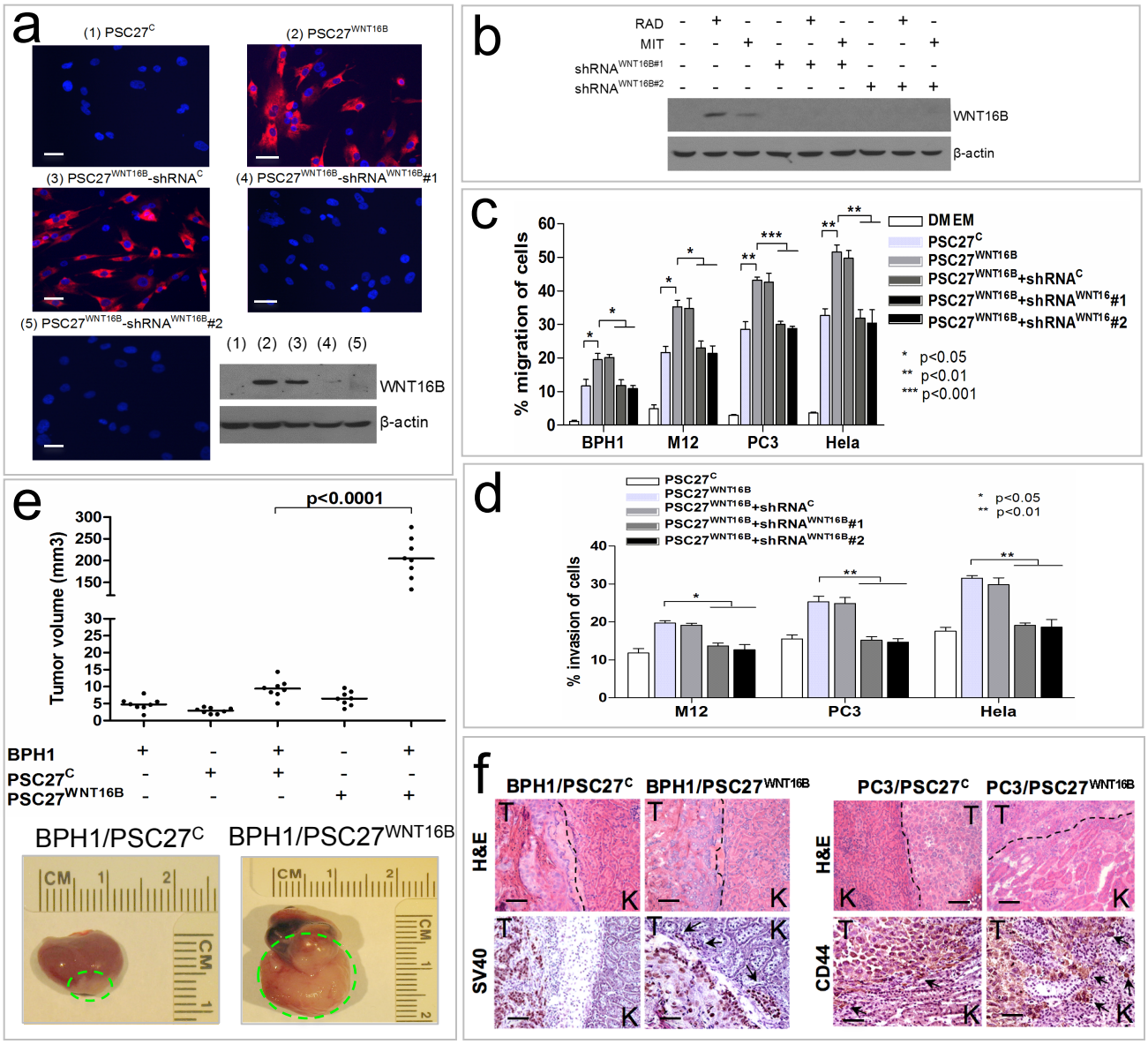

Supplementary Figure 3. Epithelial cell phenotypes are altered by fibroblast-derived paracrine-acting WNT16B. (a) Immunofluorescence confirmation of WNT16B in PSC27 cells engineered to alter WNT16B: (1) PSC27 vector control (PSC27^{C}); (2) PSC27 cells expressing WNT16B (PSC27^{WNT16B}); (3) PSC27^{WNT16B} with non-specific shRNA; (4, 5) PSC27^{WNT16B} cells with WNT16B-specific shRNAs. Scale bar, 25 µm. Below: conditioned medium from PSC27^{C} (1); PSC27^{WNT16B} (2); PSC27^{WNT16B} with control shRNA (3); and (4, 5) PSC27^{WNT16B} with WNT16B-specific shRNAs. **(b)** WNT16B shRNAs suppress the induction of WNT16B following genotoxic stress induced by irradiation (RAD) or mitoxantrone (MIT). Conditioned medium from PSC27^{WNT16B} cells promotes the migration **(c)** and invasion **(d)** of tumor cells (n=3 replicates).

(e) Fibroblast derived WNT16B promotes the growth of prostate carcinoma *in vivo*. Subrenal capsule grafts comprised of BPH1 prostate epithelial cells alone, in combination with PSC27^{C} control fibroblasts, or in combination with PSC27^{WNT16B} fibroblasts are shown. Green dashed lines denote the size of the tumor outgrowth from the kidney capsule. **(f)** Histology of subrenal capsule grafts comprised of BPH1 or PC3 prostate cells in combination with control fibroblasts (PSC27^{C}), or fibroblasts expressing WNT16B (PSC27^{WNT16B}). Dashed lines demarcate the tumor (T) from the kidney parenchyma (K). SV40 and CD44 IHC mark BPH1 and PC3 prostate epithelial cells respectively in the kidney grafts. Black arrows indicate epithelial cells invading into the kidney parenchyma. Scale bar, 150 µm.

Sun et al
Supplementary Figure 4

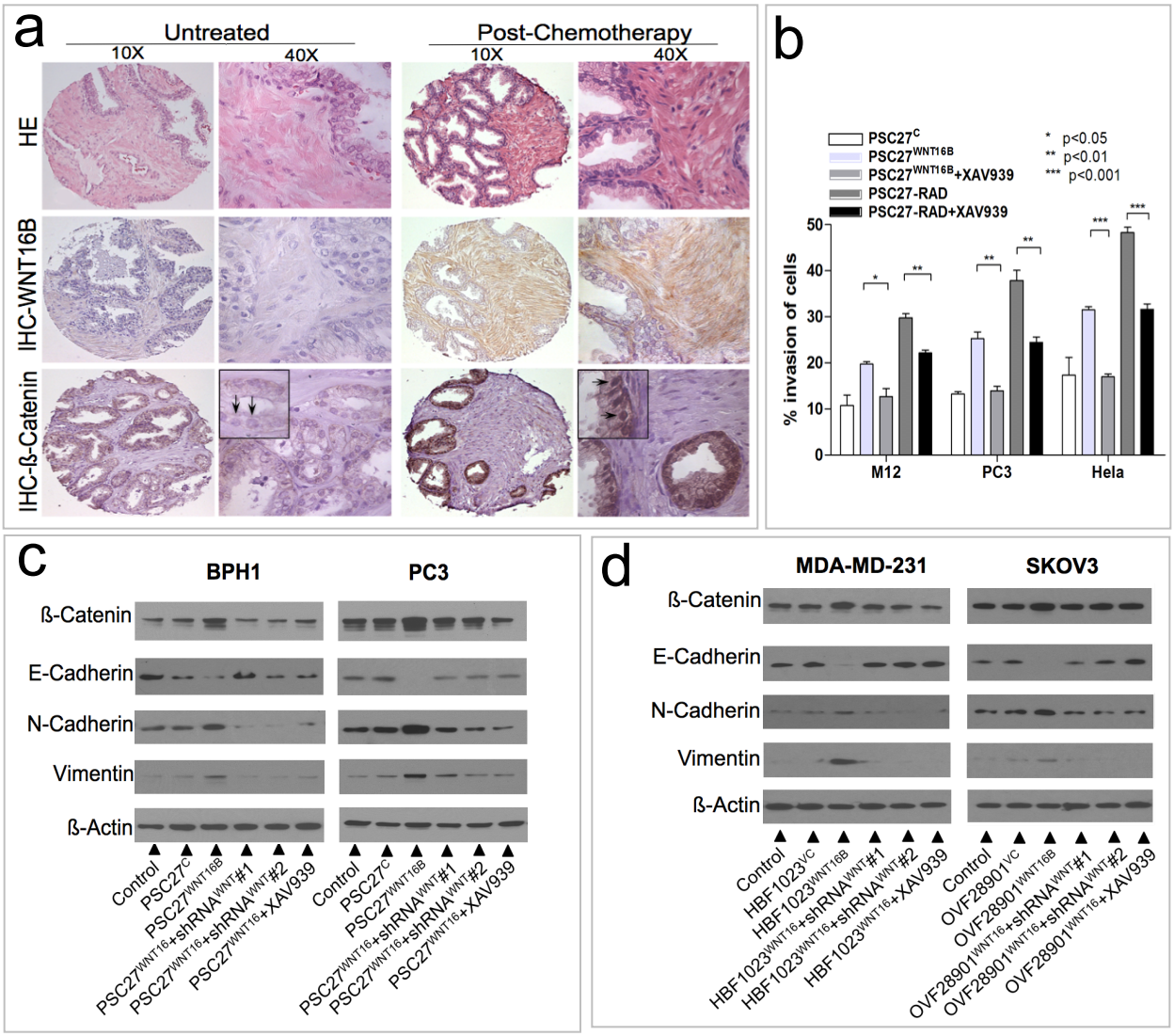

Supplementary Figure 4. Paracrine WNT16B induces a mesenchymal phenotype *in vivo.*
(a) Immunohistochemical assessment of WNT16B and β-catenin expression in human prostate cancers with and without exposure to chemotherapy. Arrows in β-catenin panels show minimal staining in cancer glands that is localized to the cytoplasm or plasma membrane in untreated tissues with intense nuclear localization in carcinoma cells following chemotherapy treatment.
(b) The β-catenin pathway inhibitor XAV939 suppresses the invasion of prostate cancer cells in response to fibroblast WNT16B and attenuates the response to the full DNA damage secretory program. Cell numbers were determined after 24 h of treatment.
(c, d) Western immunoblot analysis of proteins associated with an epithelial to mesenchymal transition. BPH1 and PC3 prostate (c), MDA MD-231 breast (d) and SKOV3 ovarian (d) epithelial cells were treated with conditioned medium from prostate (PSC), breast (HBF) or ovarian (OVF) fibroblasts expressing a vector control ($PSC27^{C}$), WNT16B ($PSC27^{WNT16B}$), WNT16B with WNT16B-specific shRNAs, or WNT16B fibroblast conditioned medium with the β-catenin pathway inhibitor XAV939.

Sun et al Supplementary Figure 5

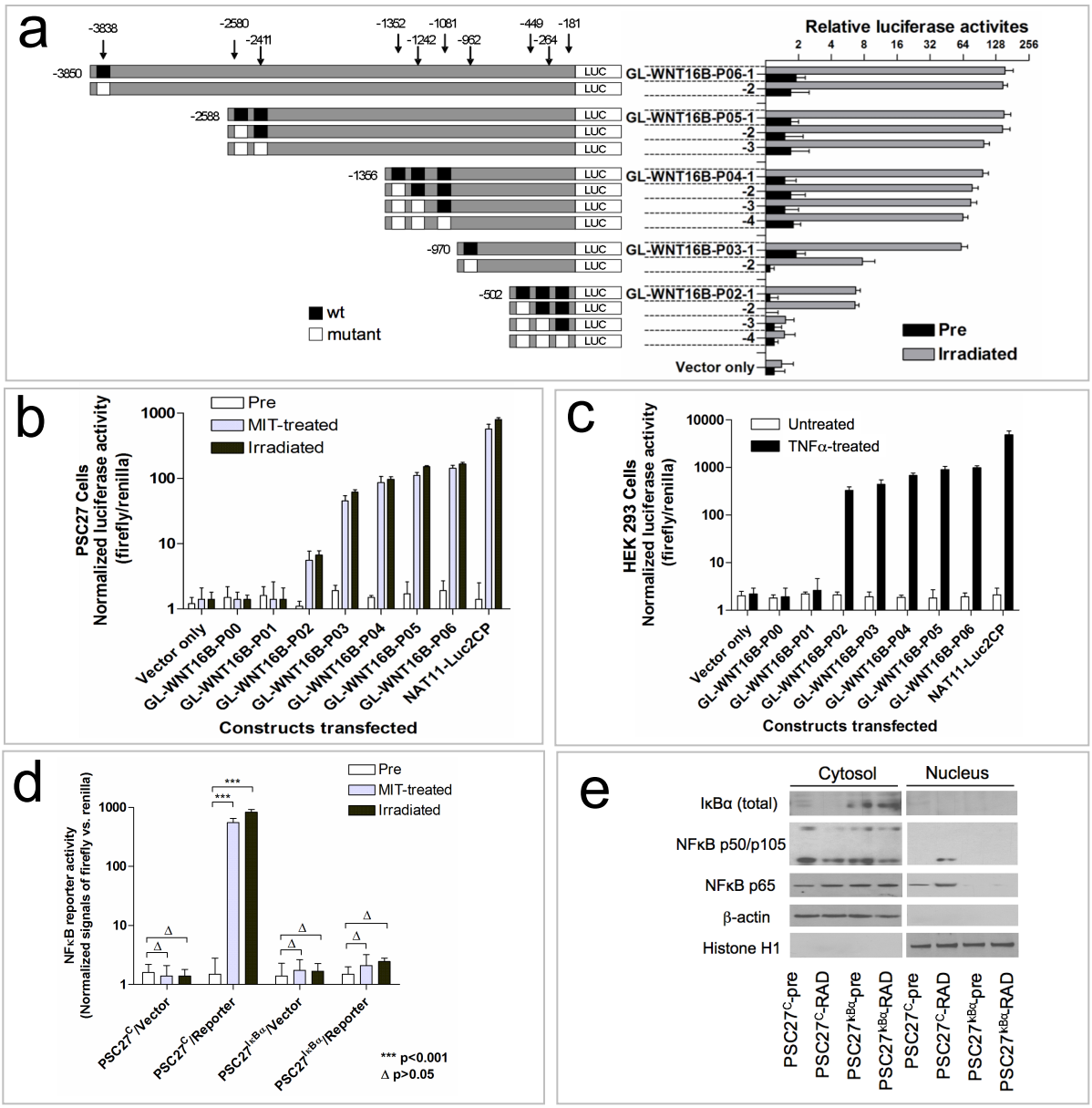

Supplementary Figure 5. WNT16B expression is regulated by NFkB. (a) Analysis of NFκB regulatory regions in the WNT16B promoter by site-directed mutagenesis. (Left) WNT16B promoter constructs for each of the 10 putative NFκB binding sites in the WNT16B promoter, denoted by -181 through -3838 bp upstream of the transcriptions start site. Black boxes = wild type sequence; White boxes = mutated NFκB binding sites. (Right) Corresponding WNT16B promoter activity with and without γ-irradiation in HEK293 cells. Data are mean ± s.d., of normalized luciferase signals (n=3). WNT16B and NFκB promoter reporter assays with genotoxic stress **(b)** and TNF-α **(c)**. Multiple NFκB binding sites maximize WNT16B promoter activity in prostate fibroblasts following irradiation or exposure to TNF-α. Constructs shown in Panel (a) were used in assays of PSC27 fibroblasts. NAT11-Luc2CP is a NFκB promoter positive control construct. **(d)** Analysis of NFκB activity following genotoxic stress with mitoxantrone or irradiation. **(e)** IκBα expression in PSC27 fibroblasts suppresses DNA damage-induced NFκB activation. Analysis of nuclear translocation of NFκB protein in prostate fibroblasts following irradiation with and without expression of mutant IκBα ($PSC27^{IκBα}$). Pre=prior to irradiation; RAD=72 h post-irradiation. β-actin and Histone H1 represent resident cytoplasmic and nuclear protein controls, respectively.

Sun et al
Supplementary Figure 6

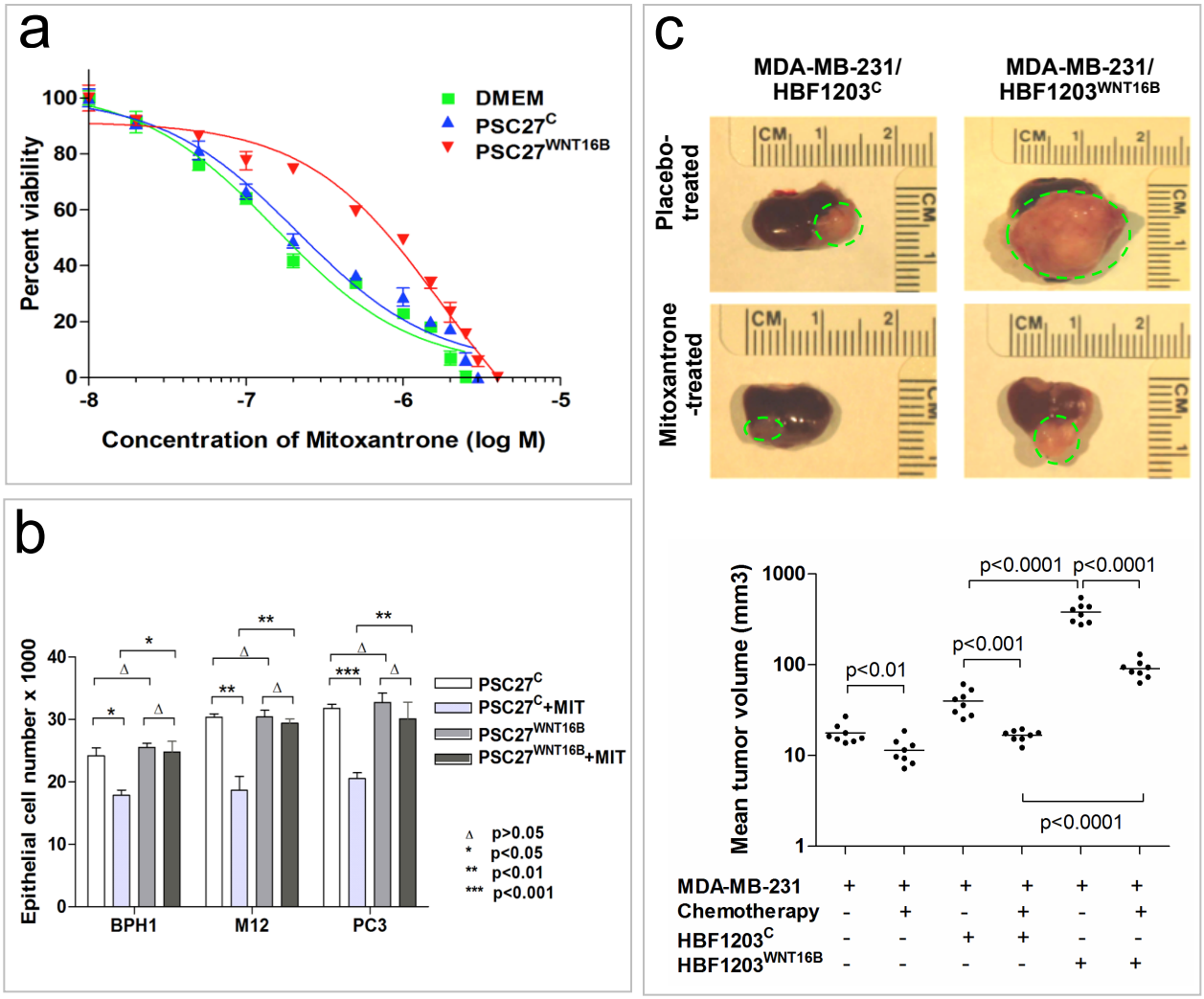

Supplementary Figure 6. Modulation of chemotherapy resistance by paracrine WNT16B.
(a) Viability of prostate cancer cells across a range of mitoxantrone concentrations with ($PSC27^{WNT16B}$) or without ($PSC27^{C}$) WNT16B in fibroblast conditioned medium. Non-linear regression curves were calculated and plotted using GraphPad Prism.
(b) Acute viability assays of epithelial cells following 12 h of exposure to IC50 concentrations of mitoxantrone and conditioned medium from PSC27 fibroblasts expressing a control vector ($PSC27^{C}$) or WNT16B ($PSC27^{WNT16B}$).
(c) Tumor volumes of subrenal capsule grafts comprised of MDA-MB-231 breast carcinoma cells in combination breast fibroblasts (HBF1203) expressing a control vector ($HBF1203^{C}$) or WNT16B ($HBF1023^{WNT16B}$) with or without treatment with 3 cycles of mitoxantrone (MIT). Tumor grafts were harvested 1 week after the 3rd cycle of treatment. Depicted are typical grafts from each treatment group with tumor masses outlined by green dashed line. Each data point represents the volume of a tumor resected from an individual mouse.

Sun et al
Supplementary Figure 7

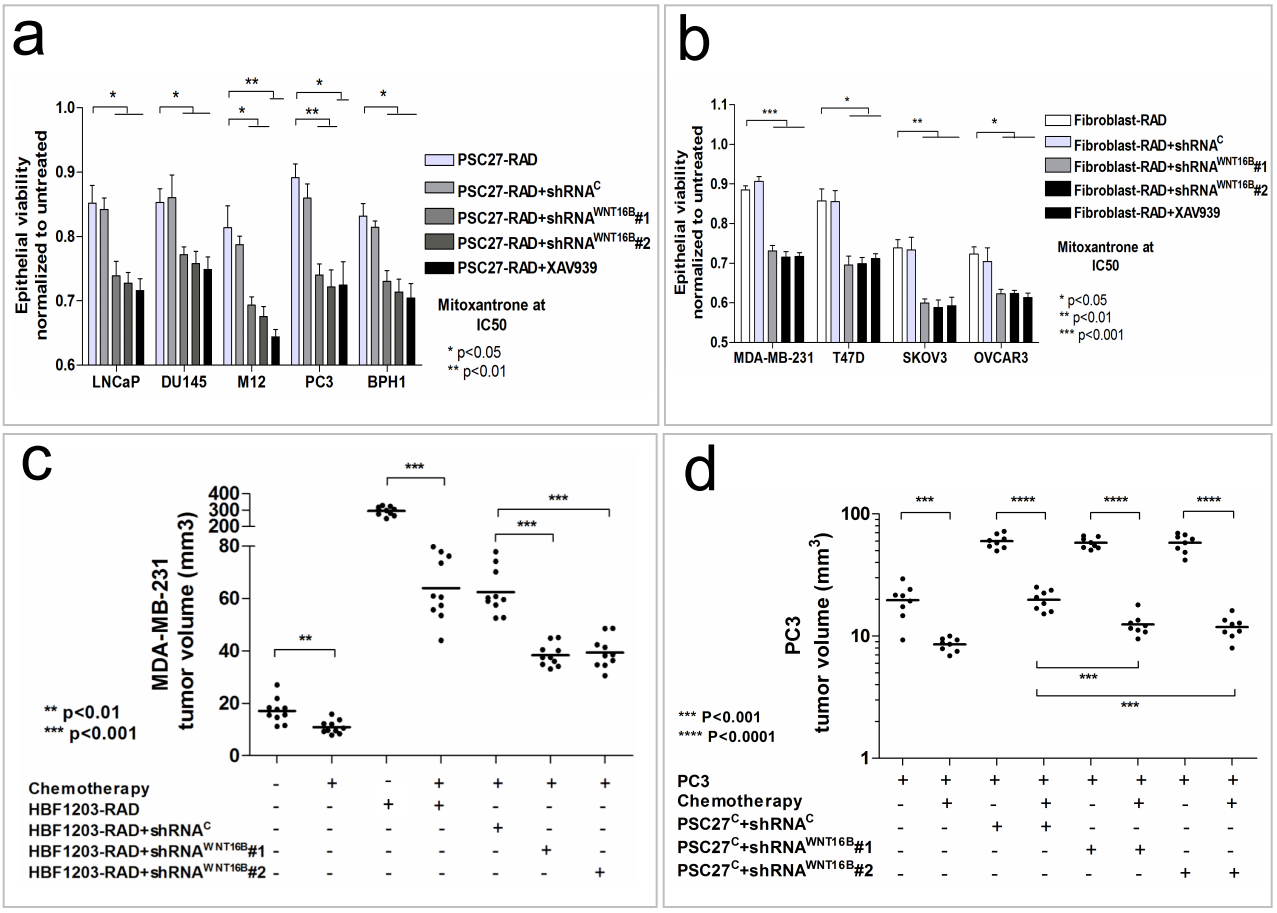

Supplementary Figure 7. Prostate, Breast and Ovarian carcinoma therapy resistance promoted by damaged fibroblasts is attenuated by blocking WNT16B or β-catenin signaling.
(a) Viability assays of prostate carcinoma cells exposed to prostate fibroblast conditioned medium and mitoxantrone chemotherapy. Epithelial cells were treated with IC50 concentrations of mitoxantrone in conditioned medium from irradiated PSC27 (PSC27^{C}-RAD) prostate fibroblasts expressing a control shRNA or WNT16B-specific shRNAs and irradiated, or with the addition of the β-catenin pathway inhibitor XAV939. Epithelial viability was determined by trypan blue counting of cells 72 h after chemotherapy. Bars represent means of 3 replicate experiments. **(b)** Viability assays of breast and ovarian carcinoma cells exposed to fibroblast conditioned medium and mitoxantrone chemotherapy. Epithelial cells were treated with IC50 concentrations of mitoxantrone in conditioned medium from irradiated breast or ovarian fibroblasts expressing a control shRNA or WNT16B-specific shRNAs and irradiated, or with the addition of the β-catenin pathway inhibitor XAV939. Epithelial viability was determined by trypan blue counting of cells 72 h after chemotherapy. Bars represent means of three replicate experiments. **(c)** *In vivo* effects of WNT16B on breast tumor responses to mitoxantrone chemotherapy. Tumors comprised MDA-MB-231 cells in combination with irradiated breast (HBF1203-RAD) fibroblasts expressing short hairpin RNAs targeting WNT16B or a vector control. Mitoxantrone was administered every 2 weeks for 3 cycles, and grafts were harvested and tumor volumes determined 1 week after the final treatment. Each datapoint represents an individual xenograft. **(d)** *In vivo* effects of mitoxantrone chemotherapy in the context of suppressing the induction of fibroblast WNT16B. Tumors comprised PC3 cells in combination with untreated prostate fibroblasts expressing a control vector (PSC27^{C}+shRNA^{C}) or shRNAs targeting WNT16B (PSC27^{C}+shRNA^{WNT16B}). Mitoxantrone was administered every 2 weeks for 3 cycles, and grafts were harvested and tumor volumes determined 1 week after the final treatment. Each data point represents an individual xenograft.

Treatment-Induced Damage to the Tumor Microenvironment Promotes Prostate Cancer Therapy Resistance Through WNT16B

Yu Sun, Judith Campisi, Celestia Higano, Tomasz M. Beer, Peggy Porter, Ilsa Coleman, Lawrence True, and Peter S. Nelson

SUPPLEMENTAL EXPERIMENTAL PROCEDURES

Cell lines and cultures. Cells of a primary normal human prostate fibroblast strain, PSC27, were cultured in prostate stromal cell (PSC) complete medium as described previously (Bavik et al., 2006). Human prostate epithelial cell lines DU145, PC3 and LNCaP were from American Type Culture Collection (ATCC, Manassas, VA) and routinely subcultured under RPMI 1640 with 5% fetal bovine serum (FBS) conditions as recommended by the vendor. The prostatic epithelial line BPH1 was kindly provided by Dr. Simon Hayward and was derived from nonmalignant prostatic tissue with benign hyperplasia, immortalized by SV40-LT antigen, and cultured as previously described [1]. The neoplastic metastatic M12 human prostate epithelial cell line was provided by Dr. Joy Ware and maintained as previously described [2]. BPH1 and M12 cells were transfected with a plasmid pIRES2-GFP, with cells passaged and subsequently flow-sorted in a FACSVantage. Cancer lines from other human cancer types including lung (A549), colon (HCT116), breast (MDA-MB-231, T47D), cervix (HeLa) and ovary (SKOV3, OVCAR3) were obtained from ATCC and cultured according to supplied instructions.

Establishment of primary fibroblast lines. Fresh human breast and ovarian tissues were acquired through IRB-approved collection protocols from discard surgical specimens. Tissue samples were washed in sterile PBS and gently agitated in RPMI/10% FBS media, with 1000 U/ml collagenase type IA. Samples were placed on the lid of a 100-mm tissue culture dish and dissected into small (2~3 mm) squares, and 5 to 10 tissue pieces were placed in the center of a 35-mm tissue culture dish or 6-well plate. A sterile 22-mm glass coverslip was placed gently

over the tissue specimens, forming a sandwich. A few drops of 4°C complete growth medium (DMEM or RPMI) was added under the coverslip. The culture was placed in a humidified 37°C, 5% CO2 incubator, with fibroblast outgrowth checked every 3 to 4 days under an inverted phase-contrast microscope, and growth medium was changed after each assessment. Upon confluenct growth, the coverslips were removed and the dish (or well) was washed twice with 4°C PBS. Trypsin/EDTA (0.25%) was used to detach cells and fibroblasts were collected by centrifugation for 10 min at 150 × g, 4°C in a 15-ml polypropylene centrifuge tube. About 3~10 × 10^4 viable cells were placed in 5 ml of fresh complete growth medium in a T25 flask. Cells attached to the new flask within 2~3 hour and began to exhibit the characteristic spindle shape within 24 hour. Medium was changed every 3~4 days until the culture was confluent, and fibroblasts were passaged two additional times following the procedure described above. To confirm the fibroblast phenotype and assess culture purity, we used immunofluorescence staining and western blot analysis with antibodies against vimentin (abcam), smooth muscle α-actin (abcam), E-cadherin (Genetex), CD44 (R&D systems) and cytokeratin 8 (Santa Cruz). The breast fibroblast line was designated HBF1023 and the ovarian fibroblast line was designated OVF28901.

Plasmids and lentiviral infection. Lentiviral agents were produced by transfecting 293FT packaging cells, with virus-containing culture medium harvested and filtered through 0.45-μm syringe filters 48 to 96 hours post-transfection. PSC27 fibroblasts were infected by exposure to virus-containing medium for 12 to 16 hours, maintained in PSC complete medium, followed by selection in puromycin. For gene-specific silencing with small hairpin RNA (shRNA), the sequences targeting WNT16B gene were cloned in a lentiviral vector pGIPZ (Thermo Scientific). Transfection of 293FT cells and subsequent infection of PSC27 cells were carried out as above, with the interference of target gene expression confirmed by immunofluorescence and immunoblot analysis.

Cell treatments with DNA damaging agents. PSC27 cells were grown until 80% confluent (PSC27-Pre) and treated with 0.6 mM hydrogen peroxide (PSC27-H_20_2), 100 µg/mL bleomycin (PSC27-BLEO) [3], 1 µM Mitoxantrone (PSC27-MIT) or ionizing-radiated by a ^{137}Cs source at 743 rad/min (PSC27-RAD). After treatment, the cells were rinsed 3x with PBS and left to recover for 3 days in PSC medium.

Immunofluorescence analysis and assessments of DNA-damage foci. Cells growing on coverslips were rinsed, subjected to fixation in 4% paraformaldehyde and permeabilization with 0.1% Triton-X100 prior to immunostaining. Primary mouse monoclonal anti-phospho-Histone H2A.X (Ser139) (clone JBW301) and secondary antibody Alexa Fluor® 488 (or 594)-conjugated F(ab')2 goat anti-mouse IgG were sequentially applied. Nuclei were counterstained with 2 µg/ml of 4',6-diamidino-2-phenylindole (DAPI) and coverslips were mounted onto glass slides. Upon visual examination of the DNA damage extent with immunofluorescence microscopy, DDR foci were recorded with a 4-category counting strategy, namely 4 classes: 0 foci, 1~3 foci, 4~10 foci, and >10 foci. Data from each cell line/treatment were averaged from a pool of 3 independent fields counting 100 nuclei per pool.

Epithelial and fibroblast co-cultures. For direct *in vitro* co-culture, BPH1-GFP cells were mixed with various proportions of PSC27 cells expressing vector control (PSC27^{C}) or WNT16B (PSC27^{WNT16B}). The cultures were incubated for 3 days after which cells were detached with trypsin and the total cell number was determined by direct counting with hemacytometer. The PSC27/BPH1-GFP proportion was determined on a FACScan using GFP fluorescence as a marker for BPH1-GFP cells. M12-GFP cells were mixed with PSC27 cells and analyzed as above. For indirect coculture, or culture of prostate epithelial cells with treated (e.g. irradiated), or WNT16-overexpressing fibroblast-conditioned medium, confluent cultures of PSC27 cells were rinsed thrice in PBS and incubated for 3 days in DMEM + 0.5% FCS. The supernatant was

harvested, filtered, concentrated and either stored frozen at –80°C or applied immediately. BPH1-GFP, PC3 and other cell lines were seeded in conditioned medium or fresh DMEM + 0.5% FBS, and grown for specific time periods and the total number of cells was determined by direct counting.

Characterization of cell phenotypes. Assays of cell proliferation were performed with the CellTiter96®AQ_{ueous} One Solution Cell Proliferation Assay (MTS) with signals captured using a 96-well plate reader. Serum-starved cells for trans-well migration and invasion assays were added to the top chambers of Cultrex 24-well Cell Migration Assay plates (8 μm size) coated with or without basement membrane extract (BM) prepared as 0.5X of stock solution. After 24 hours, migrating or invading cells in the bottom chambers were stained and plate absorbance was recorded. In the two-dimensional *in vitro* "wound healing" assay, cells were seeded before cell monolayers were incised. Photographs were taken at specific timepoints with the relative distance traveled by cells at the acellular front measured by microscopy.

Chemoresistance assays were performed using epithelial cells cultured with either DMEM and low serum (0.5% FCS) (abbreviated as "DMEM"), or conditioned medium (CM) generated from PSC27, GHF1023 or OVF28901 cells expressing vector controls, WNT16B, or siRNAs. Cells received Mitoxantrone treatment for 1 or 3 days at concentrations near individual cell line's IC_{50}. Cell viability was then assayed, and the percentage of viable cells was calculated by comparing each experiment to vehicle-treated cells. Each assay was repeated a minimum of 3 times with results reported as mean ± s.e.m.

Western analysis. Conditioned Medium (CM) or cell lysates from PSC27 cells exposed to DNA damaging treatments (radiation, Bleomycin, hydrogen peroxide, Mitoxantrone) or vehicle controls were concentrated before SDS-PAGE by trichloroacetic acid (TCA) precipitation as described (Bavik et al., 2006). After drying, the CM samples were dissolved, reduced, and sepa-

rated on a NuPAGE 4-12% gel. Primary antibodies were applied to the semi-dry-transferred blots before horseradish peroxidase (HRP)-linked secondary antibodies (Thermo Scientific, Rockford, IL) were used.

Human transcript microarray analysis. Total RNA from experimental samples was isolated using the RNeasy maxi kit (Qiagen Inc, Valencia, CA), incorporating on-column DNase treatment using the RNase-Free DNase Set (Qiagen Inc, Valencia, CA). To provide a reference standard RNA for use on two-color microarrays, we pooled equal amounts of total RNA isolated from LNCaP, DU145, PC3, and CWR22 cell lines (ATCC) growing at log phase in dye-free RPMI-1640 medium supplemented with 10% FBS (Invitrogen, Carlsbad, CA). Reference RNA was purified using TRIzol (Invitrogen, Carlsbad, CA) following the manufacturer's protocol. Reference RNA was then further purified by RNeasy maxi kit incorporating on-column DNAse treatment using the RNase-Free DNase Set. Experimental total RNA samples were amplified one round while the reference RNA was amplified two rounds using the Ambion MessageAmp aRNA Kit (Ambion Inc, Austin, TX), incorporating amino-allyl UTP into amplified antisense RNA. Sample quality and quantity were assessed by agarose gel electrophoresis and absorbance at A260 and A280 using the Nanodrop 1000 spectrophotometer (Thermo Fisher Scientific Wilmington, DE.)

Amplified amino-allyl aRNA (825 ng) from each experimental sample was labeled with Cy3 fluorescent dye (reference amino-allyl aRNA was labeled with Cy5) and hybridized to Agilent 44K whole human genome expression oligonucleotide microarray slides (Agilent Technologies, Inc., Santa Clara, CA) following the manufacturer's suggested protocols. Fluorescence array images were collected for Cy3 and Cy5 using the Agilent DNA microarray scanner G2565BA (Agilent Technologies, Inc., Santa Clara, CA), and Agilent Feature Extraction software was used to grid, extract, and normalize data. Spots of poor quality or average intensity levels <300 were removed from further analysis. The Significance Analysis of Microarray (SAM) method [4] was

used to analyze expression differences between groups. Unpaired, two-sample t tests were calculated for all probes passing filters and controlled for multiple testing by estimation of q-values using the false discovery rate (FDR) method. These results were reduced to unique genes by eliminating all but the highest scoring probe for each gene.

RNA isolation and quantitative RT-PCR. Cell cultures and human tissue samples were individually homogenized in Trizol (Invitrogen, Carlsbad CA) and total RNA was isolated using the RNeasy Kit (Qiagen Inc, Valencia, CA). RNA was quantitated in a Gene-Spec III spectrophotometer (Hitachi, Tokyo), and amplified using the MessageAmp RNA amplification kit (Ambion). cDNA was generated by a reverse transcription reaction, and quantitative PCR (qRT-PCR) analyses were performed in triplicate using an Applied Biosystems 7700 sequence detector with approximately 5 ng of cDNA, 1 μM of designated primer pairs and SYBR Green PCR master mix (Applied Biosystems, Foster City, CA). The mean cycle threshold (Ct) for each gene was normalized to levels of RPL13A in the same sample (delta Ct). Unpaired two sample t-tests were used to determine differences in mean delta Ct's between treatment groups. The fold change was calculated by the delta-delta CT method (fold = 2^{DDCt}). P values < 0.05 were considered significant.

Analyses of human clinical biospecimens. Patients with high-risk localized prostate cancer were enrolled and treated on a phase I–II clinical neoadjuvant chemotherapy trial at the Oregon Health & Science University, Portland VA Medical Center, Kaiser Permanente Northwest Region, Legacy Health System, and University of Washington [5]. Patients provided signed informed consent approving the use of their tissues for research purposes. From each patient, prostate biopsies were obtained prior to chemotherapy. At the time of radical prostatectomy following chemotherapy, cancer-containing tissue samples were obtained and snap-frozen in liquid nitrogen. Frozen sections (7 μm) were cut from OCT blocks, stained with Mayer's hematoxylin, de-

hydrated in 100% ethanol and xylene, and used for laser-capture microdissection (LCM) using an Arcturus PixCell IIe microscope (Arcturus, Mountain View, CA). Stroma, cancerous epithelium, benign epithelium, and stroma from untreated biopsy and post-treated prostatectomy specimens were captured separately and the histology of acquired cells was verified by review of H&E-stained sections from each sample and review of the LCM images.

Samples of breast carcinoma and ovarian carcinoma were collected under IRB-approved protocols. Ovarian and breast cancer specimens were selected based on either no treatment prior to surgical resection or genotoxic chemotherapy (e.g. cisplatin) prior to surgical resection.

Tissue microarrays: (TMA's) were constructed using prostates from 2 sets of patients with prostate adenocarcinoma - 50 patients (median age 63 years old; range 62 to 74 y.o.) who received neoadjuvant chemotherapy (Mitoxantrone and docetaxel) prior to radical prostatectomy and 30 patients (median age 61 years old; range 45 to 77 y.o.) who had no history of neoadjuvant chemotherapy prior to radical prostatectomy. Details of the neoadjuvant chemotherapy trial have been published. Duplicate cores from each set of radical prostatectomies were used in the TMAs. Carcinoma was confirmed in sections adjacent to those used for WNT16B immunostaining by immunostaining for a basal cell marker. An antibody to basal cell proteins high molecular weight keratins 1, 5, 10 and 14 (a mouse monoclonal antibody raised human stratum corneum; product number MS-1447-R7 clone 34betaE12, Thermo Fisher Scientific) was used in an indirect immunoperoxidase procedure.

Immunohistochemistry: Antibodies to WNT16B (a mouse monoclonal antibody raised against human WNT16B recombinant protein; product number 552595 clone F4-1582, BD Pharmingen) and anti-β-catenin (Clone 14/Beta-Catenin, BD Transduction), were used at dilutions of 1:16,000 or 1:1000, respectively. These titers were selected to minimize nonspecific staining and specificity was confirmed by omission of the primary antibody. Immunolocalization was done using an indirect three-step avidin-biotin-peroxidase method. In brief, deparaffinized sections were rehydrated in phosphate-buffered saline. Sections were then incubated sequen-

tially in solutions of 5 % albumin in PBS, 10 % hydrogen peroxide in water, primary antibody, secondary anti-mouse IgG (biotinylated anti-mouse IgG (BA-2000, Vector Labs, Burlingame, California) at 1:500 in PBS, and avidin-biotin-peroxidase solution (Vectastain ABC Elite kit at 1:100 in PBS, Vector Labs, Burlingame, CA) with interval washes in phosphate buffered saline. Reaction product was detected by incubating sections in a solution of the 0.05% diamino-benzidine and 0.3% hydrogen peroxide for 7 minutes. Sections were briefly counterstained with hematoxylin.

Interpretation of immunohistochemical stains: The level of expression of WNT16B by prostate fibromuscular stromal cells in each core of each TMA was recorded on a 4-point scale as 3 “intensely”, 2 “moderately”, 1 “faintly/equivocally” or 0, for which there was no expression by any stromal cells. Statistical analysis testing the probability that there was unlikely to be a difference in expression level by the 2 types of patients (those who received neoadjuvant chemotherapy and those who did not receive neoadjuvant chemotherapy) was performed using 2-sample unpaired t-tests or logistic regression as previously described [6]. Analyses of WNT16B staining in breast and ovarian carcinoma samples followed these procedures.

Biochemical recurrence-free survival analysis. Prostate cancer patients treated with neoadjuvant chemotherapy were partitioned into 3 groups based on stromal WNT16B expression determined by IHC: those with WNT16B average score higher than and equal to 0 but less than 1; those with WNT16B average score higher than and equal to 1 but less than 2; and those with WNT16B average score higher than and equal to 2 but less than 3. Clinical outcome data were collected following surgical prostatectomy, specifically measures of serum prostate specific antigen (PSA) as a metric of disease recurrence. Biochemical relapse was defined as a confirmed serum PSA concentration > 0.4 ng/ml (Garzotto et al., 2010). Kaplan-Meier survival curves were plotted with the program GraphPad Prism, with p-value calculated and output designated as percent biochemical relapse-free survival. Of the 55 patients enrolled in the Phase I/II clinical study, 49 had cores present on the TMA and 6 patients had frozen specimens em-

bedded in optimal cutting temperature (OCT). The positive control for WNT16B expression was PSC27-RAD cells and the negative control was IgG isotype antibody.

NFκB studies. To assess the WNT16B responses due to inhibition of NFκB nuclear translocation, the retroviral construct encoding a mutant form of IκBα, pBabe-Puro-IκBα-Mut (super repressor) that harbors two IKK phosphorylation sites genetically modified as S32A and S34A [7], was used for retroviral production with the PHOENIX packaging cell line. Infections of PSC27 fibroblasts were performed serially using drug selection (2 μg/ml of puromycin) to isolate cell populations. The established cell strain was subsequently subjected to ionizing radiation or MIT. Conditioned medium was collected as described above and used to treat epithelial cells, and gene expression was assessed by qRT-PCR or Western blot.

Analyses of cell proliferation, migration, invasion and chemotherapy resistance. All assays were performed at least three times and reported as mean values. Assays of cell proliferation were performed with the CellTiter96®AQ_{ueous} One Solution Cell Proliferation Assay (MTS) with signals captured using a 96-well plate reader or by direct counting using a hemacytometer. For trans-well migration and invasion assays, serum-starved cells in serum-free medium were added to the top chambers of Cultrex 24-well Cell Migration Assay plates (8 μm size) coated with or without basement membrane extract (BM) prepared as 0.5X of stock solution. CM from fibroblasts or regular epithelial media containing 10% fetal calf serum (FCS) were added to the bottom chambers. Migrating or invading cells in the bottom chambers were stained and plate absorbance was recorded at 485/520 nm emission. Each assay was performed in triplicate and measured at 24 hour time points over 3 days and presented as the average absorbance of migrating cells and invading cells, with human HeLA cervical cancer cell line (ATCC) used as a reference positive control.

For the two-dimensional *in vitro* "wound healing" assay, cells were seeded, allowed to establish growth and high-density areas were incised. Detached cells were removed and fresh medium was added. Photographs were taken at 0, 12 and 24 h, and the relative distance traveled by the cells at the acellular front was measured by microscopy.

For chemoresistance assays, various neoplastic epithelial cells were cultured with either DMEM of low serum (0.5% FBS) only (abbreviated as "DMEM"), or CM generated from PSC27, HBF1023 or OVF28901 in various states (e.g. WNT16B overexpression, WNT16B knockdown, irradiated). Cells received Mitoxantrone treatment for 1 or 3 days at a range of concentrations bracketing individual cell line's IC_{50} levels. Cell viability was assayed by MTS or direct counting with trypan blue, and the percentage of viable cells was calculated by normalizing absorbance of each experiment to untreated cells. To make assess the influence of WNT16B across a range of MIT concentrations, a series of drug concentrations were applied bracketing the IC50 dose, with percent survival plotted against MIT dose at a 3-day time point. Non-linear regression curves were plotted using GraphPad Prism.

For apoptosis assays, 0.2×10^6 PC3 cells were dispensed into 6-well culture plates and cocultured with media conditioned from PSC27 sublines. Twelve hours later, Mitoxantrone was added to the media at the IC50 concentration of the PC3 line, with distilled water applied in parallel as control. To measure cell apoptosis, lysates were prepared 24 hours post treatment from each group, and apoptosis quantitated using a Caspase-Glo 3/7 assay (Promega) that luminescently measures caspase-3 and -7 activities against a tetrapeptide sequence DEVD that is cleaved to release aminoluciferin,upon apoptosis in cultures. For the morphological analysis, bright field pictures were taken for PC3 cells with inverted phase-contrast microscopy.

TOPFLASH reporter assay and ß-catenin inhibition. Epithelial cells were transfected with the standardized pair of Super16×TOPFLASH and Super16×FOPFLASH (Addgene), each with a Renilla control luciferase plasmid applied for signal normalization. Empty vector pDNA3.1 was

used as control plasmid to adjust for equal DNA concentrations per transfection. A construct encoding the full-length sequence of β-catenin was used as positive control of the canonical Wnt signaling pathway. Luciferase assays were performed using a Dual-Luciferase Reporter Assay kit, and fold induction for each cell line was calculated as normalized relative light units of TOPFLASH divided by those of FOPFLASH. To inhibit the ß-catenin pathway, a small molecule compound XAV939 (Miltenyi Biotec) (Huang et al., 2009) (0.25~0.50 μM) was applied to cultures of epithelial cells treated with conditioned medium from various fibroblast manipulations and with MIT chemotherapy.

WNT16B promoter analyses. A 4000 bp region immediately upstream of the human WNT16B gene (Genbank accession NM_016087.2) was analyzed for core NF-κB binding sites using the Consite computerized DNA-binding motif search program. Three PCR primer sets were designed to amplify small regions within the proximal promoter sequence [primer set #1 (-502 to -201) forward 5'-CAGGAAAGGTCATGACACACC-3', reverse 5'- AGAGCAGCCTGGGGATCT-3'; primer set #2 (-947 to -618) forward 5'- TCTCAGGGACTGCAGGAAAT-3', reverse 5'-CCCACCAACATCTGGGTTAC-3'; primer set #3 (-1356 to -1024) forward 5'-CTCCAGGGAGTACCCTGCTA-3', reverse 5'-TGTGCTCTGATCTTTTTCTCCA-3'], and two additional primer sets were employed to amplify regions within the promoters of the human IL-6 [8] (forward 5'-AAATGCCCAACAGAGGTCA-3', reverse 5'-CACGGCTCTAGGCTCTGAAT-3') and IL-8 [9] (forward 5'- ACAGTTGAAAACTATAGGAGCTACATT-3', reverse 5'-TCGCTTCTGGGCAAGTACA-3') genes, respectively, which encompass known NF-κB binding sites. ChIP assays were then performed on PSC27 cells of early passage (p8) and those that had undergone γ-irradiation at a 10-Gy dose, with detailed procedures carried out as per previously published methods [10]. A sample of formalin-fixed sheared chromatin (DNA fragments at ~500 bp in average) from these cells was used as 'input DNA' for control amplifications. Fixed

chromatin was immunoprecipitated using monoclonal mouse anti-p65 antibody and DNAs were extracted from the immunoprecipitates and amplified using the primer sets described above. Control immunoprecipitations was carried out without antibody as control, which yielded no reaction products for any of the primer sets.

The immediate 5' upstream sequences containing putative NF-κB binding elements of the WNT16B gene were amplified from genomic DNA extracted from PSC27 cells by a DNeasy Blood and Tissue kit (QIAGEN). Primer sequences are available upon request. PCR products were cloned into pCR2.1-TOPO vector (Invitrogen) and each insert was sequenced for confirmation. PCR fragments were then double-digested and subcloned into a reporter luciferase vector pGL4.22 vector. Constructs containing one or multiple mutant NF-κB binding sites were generated from the reporter vector series by site-directed mutagenesis. The NAT11-Luc2CP-IRES-nEGFP control construct that contains large copy numbers of NF-κB binding sequences and an optimized IL-2 minimal promoter as part of NFκB-activated transgene (NAT) system was kindly provided by Dr. Hatakeyama (Hokkaido University). All constructs were confirmed by DNA sequencing in both directions. Reporter vectors were co-transfected with pRL-TK vector for transfection efficiency controls and internal normalization for gene expression measurements. Cells were either treated with 20 ng/ml TNF-α for 90 min, exposed to 10 Gy γ-irradiation or 1 μM Mitoxantrone for 1 day. PSC27 line overexpressing IκBα mutant/NF-κB super repressor was tested in parallel under above conditions for luciferase signals. Luciferase activity was measured using the Luciferase Assay System and normalized luciferase activities were calculated as light units normalized to *renilla luciferase* activity present in each specimen.

Animal and xenograft studies. All animal studies were performed in accordance with protocols approved by the Institutional Animal Care and Use Committee (IACUC) of Fred Hutchinson Cancer Research Center, and were carried out in accordance with the NIH Guide for laboratory

animals. Mouse care/welfare and veterinary oversight were provided by the center animal care. ICR *SCID* mice at an age of approximately 6 weeks (~25 g body weight) were used. Rat tail collagen (high concentration, type I) was prepared before the ice-cold collagen solution was neutralized and adjusted to the proper osmolarity by adding a mixture of NaOH and x10 PBS. To prepare tissue recombinants, fibroblasts (PSC27 strain) and epithelial cells (PC3, BPH1 or MDA-MB-231) were mixed at a ratio of 1:1, with each recombinant comprised of 250,000 cells of each line. After polymerization, the cell/collagen mixture was overlaid with growth medium and incubated at 37°C for 1 hour before implantation.

Xenografting was performed under isoflurane anesthesia. A pocket beneath the back skin was formed using surgical scissors, with an oblique incision (< 1 cm) made on the capsule surface parallel and adjacent to the long axis of each kidney. Cells were injected under the capsule with a blunt 25-gauge needle and a glass Hamilton syringe via a transrenal injection, forming a starting tumor with a volume of 1~2 mm^3. The kidney was returned to the retroperitoneal space and the skin was closed with surgical staples. The growth of xenografts was assessed at weekly intervals using ultrasound instruments. Animals were sacrificed at 2-8 weeks post transplantation, based on the tumor burden and pathological progression of tested animals. Upon dissection, tumor volume (V) was measured and calculated according to the tumor length (l) and width (w) by the following formula: $V = (\pi/6) \times ((l+w)/2)^3$ [11]. Tumors were snap-frozen or processed conventionally for formalin fixation. Resulting sections were used for hematoxylin/eosin staining, and immunostaining for selected gene expression markers.

For chemoresistance studies, ICR *SCID* mice received subrenal capsule xenografts implantation according to the procedure described above. After surgery, mice were given standard laboratory diets and water *ad libitum* for 2 weeks, to allow tumor uptake and growth initiation. Starting from the 3rd week (when tumor sizes reached 4~8 mm in diameter), mice received Mitoxantrone at a dose of 0.2 mg/kg by i.p. injection, or vehicle control, on day 1 of week 3, week 5, and week 7. Between 8 and 12 mice were randomly assigned to each study arm. A total regimen of 3 2-week cycles was administered [12]. After the final treatment cycle the

regimen of 3 2-week cycles was administered [12]. After the final treatment cycle the mice were sacrificed, kidneys were removed for tumor measurement and histological analysis. The cumulative Mitoxantrone dose received per mouse was 0.6 mg/kg.

To determine the systemic effects of MIT treatment on Wnt16b expression, parallel experiments involved administering MIT or vehicle as per the treatment schema above, to cohorts of mice (n=6) without xenografts. At the completion of the 8-week treatment regimen, mice were euthanized and various tissues were rapidly resected and snap frozen or fixed in formalin. Following protein isolations, Western immunoblot analysis was performed for Wnt16b expression, as described above.

For assessments of the acute effects of chemotherapy, mice harboring xenografts of PC3 cells combined with PSC27 fibroblasts were treated with Mitoxantrone 0.2 mg/kg by i.p. injection, or vehicle control. Xenografts were collected 24 hour after treatment and tissues were processed for IHC. Apoptosis was assessed by staining with anti-caspase 3 antibody (cleaved, BioCare Medical). On adjacent sections, immunostaining with anti-γH2AX (Upstate) was performed to quantitate cells with DNA-damage.

Statistical Analysis. Analyses of microarray experiments are described above. In vitro studies of cell proliferation, viability, or invasion were performed a minimum of 3 times and data reported as ± s.e.m. Statistical analyses was performed on raw data for each group by one-way analysis of variance or a two-tailed Student's t-test. A $p<0.05$ was considered significant.

Table of PCR primers.

GENE SYMBOL[1]	GENE NAME[1]	PRIMERS	SEQUENCES
WNT16	**Wingless-type MMTV integration site family, member 16**	Forward	5'-GCTCCTGTGCTGTGAAAACA-3'
		Reverse	5'-TGCATTCTCTGCCTTGTGTC-3'
p16/ CDKN2A/ INK4A	**Cyclin-dependent kinase inhibitor 2A**	Forward	5'-GACATCCCCGATTGAAAGAA-3'
		Reverse	5'-TTTACGGTAGTGGGGGAAGG-3'
p21/ CDKN1A/ CIP1	**Cyclin-dependent kinase inhibitor 1A**	Forward	5'-GACACCACTGGAGGGTGACT-3'
		Reverse	5'-CAGGTCCACATGGTCTTCCT-3'
IL-8/CXCL8	**Interleukin 8**	Forward	5'-GTGCAGTTTTGCCAAGGAGT-3'
		Reverse	5'-CTCTGCACCCAGTTTTCCTT-3'
E-cadherin/ CDH1	**E-cadherin (epithelial)**	Forward	5'-TGCCCAGAAAATGAAAAAGG-3'
		Reverse	5'-GTGTATGTGGCAATGCGTTC-3'
N-cadherin/ CDH2	**N-cadherin (neuronal)**	Forward	5'-GACAATGCCCCTCAAGTGTT-3'
		Reverse	5'-CCATTAAGCCGAGTGATGGT-3'
VIM	**Vimentin**	Forward	5'-GAGAACTTTGCCGTTGAAGC-3'
		Reverse	5'-TCCAGCAGCTTCCTGTAGGT-3'
TWIST1	**Twist homolog 1**	Forward	5'-GTCCGCAGTCTTACGAGGAG-3'
		Reverse	5'-CCAGCTTGAGGGTCTGAATC-3'
SNAIL2	**Snail homolog 2**	Forward	5'-CTTTTTCTTGCCCTCACTGC-3'
		Reverse	5'-ACAGCAGCCAGATTCCTCAT-3'
TWIST2	**Twist homolog 2**	Forward	5'-AGCAAGAAGTCGAGCGAAGA-3'
		Reverse	5'-CAGCTTGAGCGTCTGGATCT-3'
AXIN2	**Axin2**	Forward	5'-CCTGCCACCAAGACCTACAT-3'
		Reverse	5'-CTTCATTCAAGGTGGGGAGA-3'
SP5	**Sp5**	Forward	5'-ACTTTGCGCAGTACCAGAGC-3'
		Reverse	5'-ACGTCTTCCCGTACACCTTG-3'
c-Myc/MYC	**v-myc viral oncogene homolog (avian)**	Forward	5'-TTCGGGTAGTGGAAAACCAG-3'
		Reverse	5'-CAGCAGCTCGAATTTCTTCC-3'
Cyclin D1/ CCND1	**Cyclin D1**	Forward	5'-AACTACCTGGACCGCTTCCT-3'
		Reverse	5'-CCACTTGAGCTTGTTCACCA-3'
RPL13A	**Ribosomal protein L13a**	Forward	5'-GTACGCTGTGAAGGCATCAA-3'
		Reverse	5'-CGCTTTTTCTTGTCGTAGGG-3'

[1] According to the HUGO Gene Nomenclature Committee.

Supplemental References for Methods.

1. Hayward, S.W.*, et al.* Establishment and characterization of an immortalized but non-transformed human prostate epithelial cell line: BPH-1. *In Vitro Cell Dev Biol Anim* **31**, 14-24. (1995).
2. Bae, V.L.*, et al.* Metastatic sublines of an SV40 large T antigen immortalized human prostate epithelial cell line. *Prostate* **34**, 275-282 (1998).
3. Bavik, C.*, et al.* The Gene Expression Program of Prostate Fibroblast Senescence Modulates Neoplastic Epithelial Cell Proliferation through Paracrine Mechanisms. *Cancer Res.* **66**, 794-802. (2006).
4. Tusher, V.G., Tibshirani, R. & Chu, G. Significance analysis of microarrays applied to the ionizing radiation response. *Proc Natl Acad Sci U S A* **98**, 5116-5121. (2001).
5. Beer, T.M.*, et al.* Phase I study of weekly Mitoxantrone and docetaxel before prostatectomy in patients with high-risk localized prostate cancer. *Clin Cancer Res* **10**, 1306-1311. (2004).
6. Lucas, J.M.*, et al.* The androgen-regulated type II serine protease TMPRSS2 is differentially expressed and mislocalized in prostate adenocarcinoma. *J Pathol* **215**, 118-125 (2008).
7. Boehm, J.S.*, et al.* Integrative genomic approaches identify IKBKE as a breast cancer oncogene. *Cell* **129**, 1065-1079 (2007).
8. Naugler, W.E. & Karin, M. NF-kappaB and cancer-identifying targets and mechanisms. *Curr Opin Genet Dev* **18**, 19-26 (2008).
9. Martone, R.*, et al.* Distribution of NF-kappaB-binding sites across human chromosome 22. *Proc Natl Acad Sci U S A* **100**, 12247-12252 (2003).
10. Nelson, J., Denisenko, O. & Bomsztyk, K. The fast chromatin immunoprecipitation method. *Methods Mol Biol* **567**, 45-57 (2009).
11. Anand, N.*, et al.* Protein elongation factor EEF1A2 is a putative oncogene in ovarian cancer. *Nat Genet* **31**, 301-305 (2002).
12. Alderton, P.M., Gross, J. & Green, M.D. Comparative study of doxorubicin, Mitoxantrone, and epirubicin in combination with ICRF-187 (ADR-529) in a chronic cardiotoxicity animal model. *Cancer Res* **52**, 194-201 (1992).